PFC/RR-88-3 DOE/ET 51013-247
UC-246

Spectral Analysis of ICRF Wave Field Measurements in the Tara Central Cell

L. Wang, S.N. Golovato, S.F. Horne

Plasma Fusion Center
Massachusetts Institute of Technology
Cambridge, MA 02139

December 1987

Abstract

A simple spectral analysis technique has been developed to analyse the digital signals from an array of magnetic probes for ICRF field measurements in the Tara Tandem Mirror central cell. The wave dispersion relations of both the applied ICRF and the Alfven Ion cyclotron Instability have been studied and the waves have been identified as slow in cyclotron waves. The radial profiles of field amplitude and wave vectors were also generated.

I. Introduction

Plasma heating in the Ion Cycrotron Range of Frequences (ICRF) is used in the Tara Tandem Mirror to build up and heat plasma[1,2] in the central cell. To understand the ICRF wave propagation and heating, one method is to measure by magnetic probes the wave magnetic field amplitude distribution over space and the phase of the RF wave to obtain the dispersion relation. In determining the wave amplitude and wave vector from the digitized data of the oscillating RF fields, the most often used method is by the Fourier transform of the cross correlation function.The technique is described in many articles.[3-6] Rather than using Fast Fourier Fransformation (FFT)[6] of the cross correlation, an equivalent method has been developed which is simpler and faster to process the large amount of data from experiments.

II. Spectral Analysis

Assume the B field measured at time t is decomposed to its Fourier spectrum by

$$\begin{aligned} B(t) &= \int_{-\infty}^{\infty} df B(f) e^{-2\pi i f t} \\ &= \int_{-\infty}^{0} df B(f) e^{-2\pi i f t} + \int_{0}^{\infty} df B(f) e^{-2\pi i f t} \\ &= \int_{0}^{\infty} df B(-f) e^{2\pi i f t} + \int_{0}^{\infty} df B(f) e^{-2\pi i f t} \\ &= \int_{0}^{\infty} df B^*(f) e^{2\pi i f t} + \int_{0}^{\infty} df B(f) e^{-2\pi i f t} \\ &= \int_{0}^{\infty} df |B(f)| (e^{-i\alpha(f)+2\pi i f t} + e^{i\alpha(f)-2\pi i f t}) \\ &= 2\int_{0}^{\infty} df |B(f)| cos(2\pi f t - \alpha(f)), \end{aligned} \tag{1}$$

where we have used the fact that since $B(t)$ is real

$$B^*(f) = B(-f) \tag{2}$$

and also

$$B(f) = |B(f)| e^{i\alpha(f)}. \tag{3}$$

If $|B(f)|$ is significant only in Δf and peaking at f_0, the applied frequency, we then have

$$B(t) \simeq cos(2\pi f_0 t - \alpha(f_0))2\int_{\Delta f} df|B(f)|. \tag{4}$$

On the other hand assuming the wave we are measuring is of the form

$$B(z,t) = B_0 cos(2\pi f_0 t - k(f_0)z) \tag{5}$$

and comparing with (4) we get

$$\alpha(f_0) = k(f_0)z + c, \tag{6}$$

where c is a constant,and

$$B_0 = 2\int_{\Delta f} df|B(f)|. \tag{7}$$

To get the dispersion relation $k(f)$ the method used most often is the Fourier transformation of cross correlation, which has the following properties. If we have two time dependent functions $x(t)$ and $h(t)$ the cross correlation function is defined as[6]

$$z(t) = \int_{-\infty}^{\infty} d\tau x(\tau)h(t+\tau). \tag{8}$$

We then have

$$Z(\omega) = H(\omega)X^*(\omega), \tag{9}$$

where $Z(\omega)$, $H(\omega)$ and $X(\omega)$ are Fourier transform of $z(t)$, $h(t)$ and $x(t)$ respectively. In our application, we can form a cross correlation function from the signals measured at different positions for the same shot as

$$B_{12}(t) = \int_{-\infty}^{\infty} d\tau B_1(z_1,\tau)B_2(z_2,t+\tau). \tag{10}$$

Since in general

$$\begin{aligned} B(z,t) &= \int_{-\infty}^{\infty} df B(z,f)e^{-2\pi ift} \\ &= \int_{-\infty}^{\infty} df B(f)e^{i(k(f)z-2\pi ft)}, \end{aligned} \tag{11}$$

by (10) we get

$$\begin{aligned} B_{12}(f) &= B_{12}(f) \\ &= |B_{12}(f)|e^{i\alpha_{12}(f)} \\ &= B_1(z_1,f)B_2^*(z_2,f) \\ &= |B_1(f)||B_2(f)|e^{ik(f)(z_1-z_2)}. \end{aligned} \tag{12}$$

Since $z_1 - z_2$ is known $k(f)$ can now be obtained from the phase of the cross correlation spectrum.

There are two ways to get $B_{12}(f)$. The first is to perform the integration (11) first and then do the fast Fourier transform. The second is to fast Fourier transform $B_1(z_1,t)$ and $B_2(z_2,t)$ first respectively and then multiply them to get the spectrum $B_{12}(f)$. The second way is much faster than the first one by avoiding the time consuming integration. Actually, we do not even have to get $B_{12}(f)$ by multiplication of $B_1(z_1,f)$ and $B_2(z_2,f)$ because of formula (6). We can simply read off $\alpha_1(f_0)$ and $\alpha_2(f_0)$ respectively and substract them to get $k(f_0)$. We can determine the wave amplitude simultaneously from the fluctuating spectrum by using the formula (7) via integration.

However, due to the other fluctuations in plasma such as instabilities and harmonic genreration, the spectrum is not always clean. This leads to the difficulty in searching for Δf automatically by computer program. It also takes time to do the integration of (7).

Another equivalent method exists thanks to the discreteness of the digital Fourier analysis. Suppose we have a given sinusoidal wave

$$B(t) = B_0 sin(2\pi f_0 t + \alpha). \tag{13}$$

Its discrete Fourier transform has to be windowed. Suppose the window is square between

sampling time t_1 and t_2. The Fourier spectrum is then

$$\begin{aligned} B(f) &= \int_{t_1}^{t_2} dt B_0 sin(2\pi f_0 t + \alpha) e^{2\pi i f t} \\ &= \frac{B_0}{2i} \int_{t_1}^{t_2} dt (e^{i(2\pi(f_0+f)t+\alpha)} - e^{-i(2\pi(f_0-f)t+\alpha)}) \\ &= \frac{B_0 e^{i\alpha}}{2i2\pi i(f+f_0)} (e^{2\pi i(f+f_0)t_2} - e^{2\pi i(f+f_0)t_1}) \\ &\quad - \frac{B_0 e^{-i\alpha}}{2i2\pi i(f-f_0)} (e^{2\pi i(f-f_0)t_2} - e^{2\pi i(f-f_0)t_1}) \end{aligned} \tag{14}$$

$B(f)$ peaks at $f = f_0$ where

$$B(f_0) = \frac{B_0 e^{i\alpha}(t_1 - t_2)}{2i} \tag{15}$$

from which we obtain B_0 as

$$\begin{aligned} B_0 &= \frac{2|B(f_0)|}{|t_1 - t_2|} \\ &= \frac{2|B(f_0)|}{\Delta t} \end{aligned} \tag{16}$$

One can also get this from (11) since for any spectrum $\Delta f \simeq 1/\Delta t$.

This says that for a good sinusoidal wave the amplitude is equal to the absolute value of its Fourier spectrum peak divided by half of the sampling time interval. This technique requires well seperated discrete modes in the Fourier spectrum in order to evaluate $B(f_0)$ accurately.

A program which reads the experimental data, performs the fast Fourier transform, and outputs the wave amplitudes and phases has been written in IDL.[7] IDL is a software system for the interactive analysis, reduction, and display of scientific data. The program listing is shown here.

```
;*************************************************************************
; This program inputs data from TARA data base and outputs the amplitude
; and the phase at the peak frequency.
;
;*************************************************************************
CLOSE,1
FILE='DENSITY.SCAN'
SHN=INTARR(100)
FOR M=1,27 DO BEGIN                    ;****************************************
SHN(M)=14883+M                         ;SHOT NUMBERS
ENDFOR                                 ;****************************************
T1=.0300                               ;SAMPLING TIME INTERVAL
T2=.030256                             ;****************************************
N1=8191                                ;NUMBER OF DATA POINTS
N2=N1+1                                ;****************************************
PI=ACOS(-1.)
PI2=2.*PI
DLT=T2-T1
DT=DLT/FLOAT(N2)
Q=1.E6                                 ;FREQUENCY SCALE MHZ
FREQ=32./FLOAT(N1)*FINDGEN(N2)         ;32 MEGAHERTS DIGITIZER
SS=(T1/DLT)-FIX(T1/DLT)
HFF=(SS*FINDGEN(N2))-FIX(SS*FINDGEN(N2))
F11=3.45
F12=3.50
S=['1','2','3','4','5','6']
OPENW,1,FILE                           ;****************************************
FOR K=1,27 DO BEGIN                    ;
SHOTN=FIX(SHN(K))                      ; READ IN DATA
PRINTF,1,'SHOT#=',SHOTN                ;
FOR J=1,6 DO BEGIN                     ;
SIG='CC_BDOT_R'+S(J-1)                 ;
DUMMY=SET_SHOT(SHOTN)                  ;
Y=DATA(SIG)                            ;
T=DATA('CC_BDOT_R1_TM')                ;****************************************
HF1=FFTRC(Y)                                        ;IMSL FFT
HF1=COMPLEX(COS(PI2*HFF),SIN(PI2*HFF))*HF1          ;TAKES CARE OF PHASE
AP=ABS(HF1)
PH=FLOAT(ATAN(HF1))
HF1=0
MX=MAX(AP(WHERE((FREQ GE F11) AND (FREQ LE F12))))  ;SEARCH FOR PEAK
AMP=2.*MX/FLOAT(N2)                                 ;GET THE PEAK AMPLITUDE
FS1=PH(WHERE(AP(WHERE(FREQ LE 6.)) EQ MX))
FM1=FREQ(WHERE(AP(WHERE(FREQ LE 6.)) EQ MX))
OMEGAPEAK=FM1(0)
PHASE=(PI-FS1(0))*180/PI                            ;GET THE PEAK PHASE
PRINTF,1,SIG,'  AMP=',AMP, $                        ;OUTPUT
'  PHASE=',PHASE
ENDFOR
ENDFOR
CLOSE,1
END
```

III. Experimental Results

An array of magnetic probes has been used to measure the ICRF fields in the central cell of the Tara Tandem Mirror. Each probe consists of three orthogonal six turn coils to measure all three field components simultaneously. They are Faraday shielded, center-tapped, and encased in insulator to ensure that signals are due solely to ICRF magnetic fields. The probe frequency response 3 dB point is 14 MHz. The probes have been calibrated in Gauss and the instrumental phase shifts have been taken into account. The 3.47 MHz ICRF is excited by a slot antena located on a bump of mirror ratio 1.7 at the central cell midplane and propagates to a beach resonance where

$$\omega \rightarrow \omega_{ci} \equiv \frac{eB}{mc} \tag{17}$$

on either side of the bump. The probes are located along the beach at 3 axial and 3 azimuthal positions.

Experiments were also done with and without a divertor at the central cell midplane. The purpose of the divertor is to stablize the plasma. It creates a magnetic null at the midplane near the plasma edge which may affect the wave propagation since there will be a resonance in this region.

A typical specrtum of the azimuthal component of the RF magnetic field, B_θ, is shown in Fig. 1. The observed fields are (1) applied ICRF at 3.47 MHz and (2) plasma generated Alfven Ion Cycrotron (AIC) instability modes[9] along with harmonics and non-linear combinations of these principal modes. The measured dispersion relations of the ICRF and AIC waves are shown in Fig. 2 and 3 respectively. They both satisfy the slow wave dispersion relation for infinite homogeneous cold plasma[8]

$$k_\parallel = \frac{\omega}{\omega_{ci}} \frac{\omega_{pi}}{c} \frac{1}{(1-(\omega/\omega_{ci})^2)^{1/2}} \tag{18}$$

where $\omega_{pi} \equiv (4\pi ne^2/m)^{1/2}$. Figure 4 shows the radial profiles of the ICRF amplitude, B_θ, at three different azimuthal angles with and without magnetic divertor. The divertor has

little effect on the radial profiles of RF magnetic fields. The B field vanishes at plasma edge and peaks at a radius of 10 to 15 cm. The radial profiles show some azimuthal dependence.

The left and right circularly polarized wave profiles are shown in Fig. 5. There is no strong polarization effect. In Fig. 6 we can see that B_r components are flat and B_θ peaks at $r \approx 15cm$. The central cell divertor has little effect on them.

We have also investigated the azimuthal wave number $k_\theta(r)$ which is defined by

$$B \sim e^{i(k_\theta(r)\theta - k_\parallel(r)z)}. \tag{19}$$

Figure 7 shows k_θ is similar with and without divertor and has radial structure with mixed m mode. That is, it is not a simple $m = +1$ or $m = -1$ mode.

The radial profiles of the axial wave number $k_\parallel$ defined in (19) are shown in fig. 8. $k_\parallel$ increases as ω approaches ω_{ci}. The slow wave is seen in the plasma core and the fast wave (small $k_\parallel$) only at extreme edge (beyond limiter).

Fig. 9 displays the B_θ field amplitudes vs ω/ω_{ci}. B_θ increases as $\omega/\omega_{ci} \rightarrow 1$ as expected from Eq. (19).

Finally the scaling of $k \parallel$ with gas fueling rate is shown in Fig. 10. $k \parallel$ increases as the fueling is increased in agreement with Eq. (18) where $\omega_{pi} \sim \sqrt{n}$ so $k_\parallel \sim \sqrt{n}$.

Acknowledgement

The authors would like to thank Richard C. Myer, and John Machuzak for helpful disscusions.

References

[1]R. S. Post, et al, *Plasma Physics and Controlled Thermolnuclear Research Conference Proceedings*, Kyoto, 13-20 November 1986, pp. 251-262, vol 2.

[2]S. N. Golovato, et al, AIP Conference Proceedings 159, *Applications of Radio-frequency Power to Plasmas*, Seventh Topical Coference, Kissimmee,Fl 1987, Editors , S. Bernabi, et al, pp 254-257.

[3]E. B. Hooper,Jr., Plasma Physics **13**, 1 (1971).

[4]M. Bernard, et al, *Plasma Physics and Controlled Thermalnuclear Research Conference Proceedings*, Novosibirsk, 1-7 August 1968, pp. 715-733, vol 1.

[5]D. E. Smith, et al, IEEE Transactions on Plasma Science, vol. PS-2 Dec 1974.

[6]E. O. Brigham, *The Fast Fourier Transform*, N.J. Prentice-Hall, 1974.

[7]Research Systems,Inc. 2012 Albion Street Denver, CO80207, *Introduction to IDL*, Feb 1,1987.

[8]T. H. Stix, *The Theory of the plsma waves*, McGraw-hill, 1962, p. 35.

[9]G. R. Smith, Phys. Fluids **27**, 1499 (1984).

Figures

FIG. 1. A typical spectrum of the azimuthal component of the RF magnetic field, B_θ.

FIG. 2. The dispersion relation of the applied ICRF wave. The solid line is the dispersion relation of the slow Alfven wave for the infinite homogeneous cold plasma. i.e.

$$k_\parallel = \frac{\omega}{\omega_{ci}} \frac{\omega_{pi}}{c} \frac{1}{(1-(\omega/\omega_{ci})^2)^{1/2}}$$

FIG. 3. The dispersion relation of the plasma generated AIC mode. The solid line represents the same formula as in fig. 2.

FIG. 4. The radial profiles of the amplitude of B_θ at three different azimuthal angles.

FIG. 5. The radial profiles of the amplitude of left circular B_+ and right circular B_- polarized wave at two different ω/ω_{ci} positions.

FIG. 6. The radial profiles of the amplitude of radial component B_r and azimuthal component B_θ waves with and without divertor.

FIG. 7. The radial profiles of azimuthal wave number at two different angles with and without divertor.

FIG. 8. The radial profiles of axial wave numbers for B_θ at two ω/ω_{ci} positions with and without divertor.

FIG. 9. The B_θ fields vs ω/ω_{ci}.

FIG. 10. The scaling of axial wave number with density.

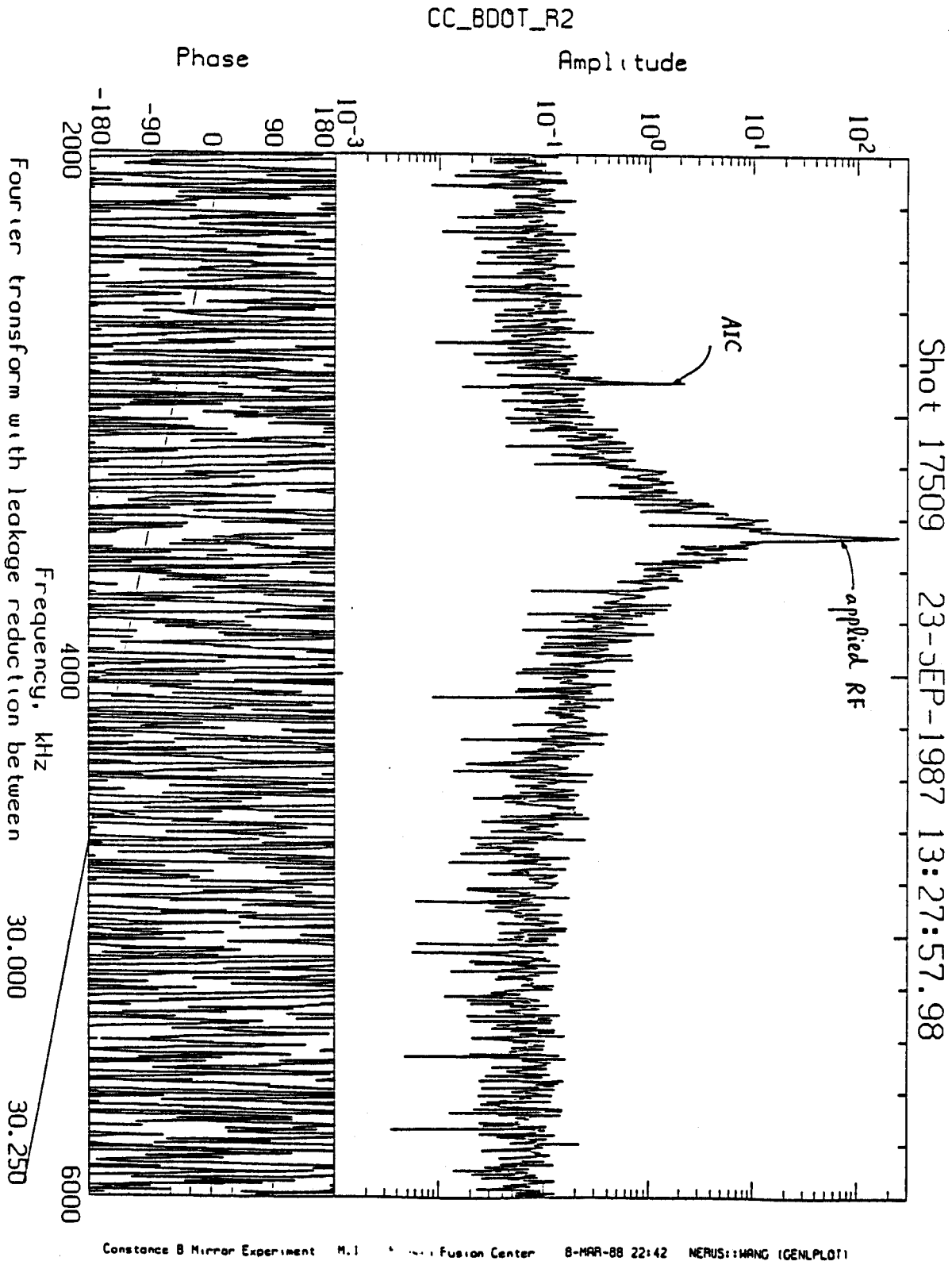
CC_BOOT_R2
Phase
Amplitude
-180
-90
0
90
180
10^{-3}
10^{-1}
10^{0}
10^{1}
10^{2}
2000
4000
6000
AIC
applied RF
Shot 17509 23-SEP-1987 13:27:57.98
Fourier transform with leakage reduction between 30.000 30.250
Frequency, kHz
Constance B Mirror Experiment M.I Fusion Center 8-MAR-88 22:42 NERUS::WANG (GENLPLOT)

Figure 1

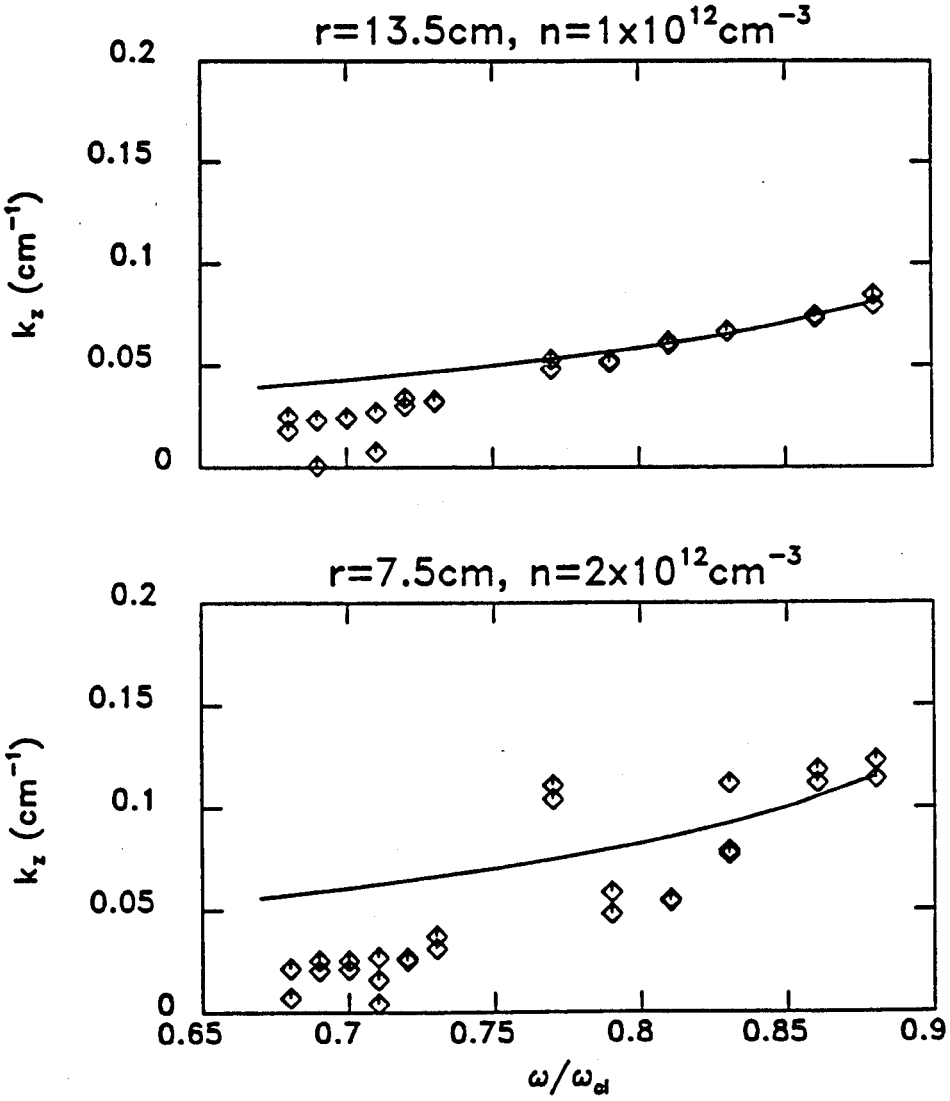
r=13.5cm, n=1x10^12cm^-3
0.2
0.15
0.1
0.05
0
k_z (cm^-1)
r=7.5cm, n=2x10^12cm^-3
0.2
0.15
0.1
0.05
0
k_z (cm^-1)
0.65
0.7
0.75
0.8
0.85
0.9
ω/ω_ci

Figure 2

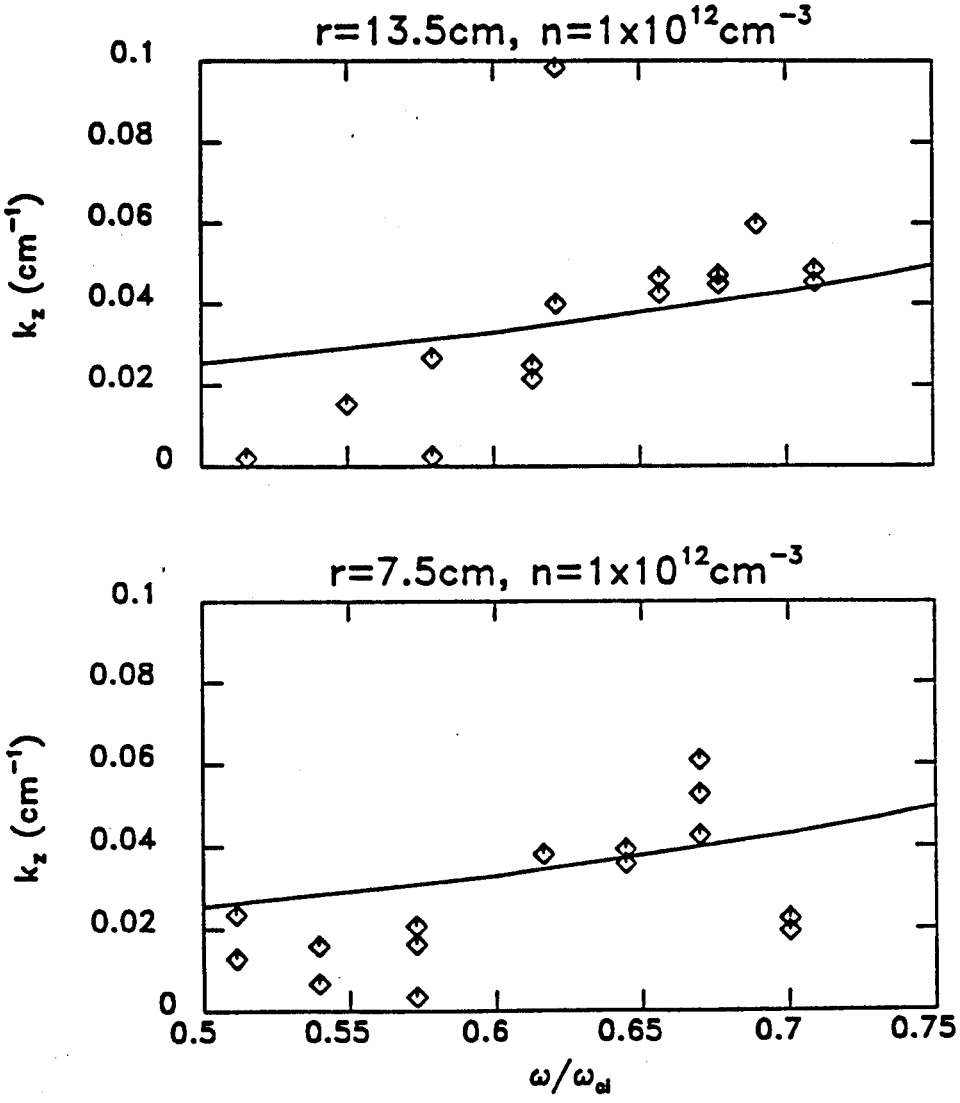
r=13.5cm, n=1x10^12cm^-3
0.1
0.08
0.06
0.04
0.02
0
k_z (cm^-1)
r=7.5cm, n=1x10^12cm^-3
0.1
0.08
0.06
0.04
0.02
0
k_z (cm^-1)
0.5
0.55
0.6
0.65
0.7
0.75
ω/ω_ci

Figure 3

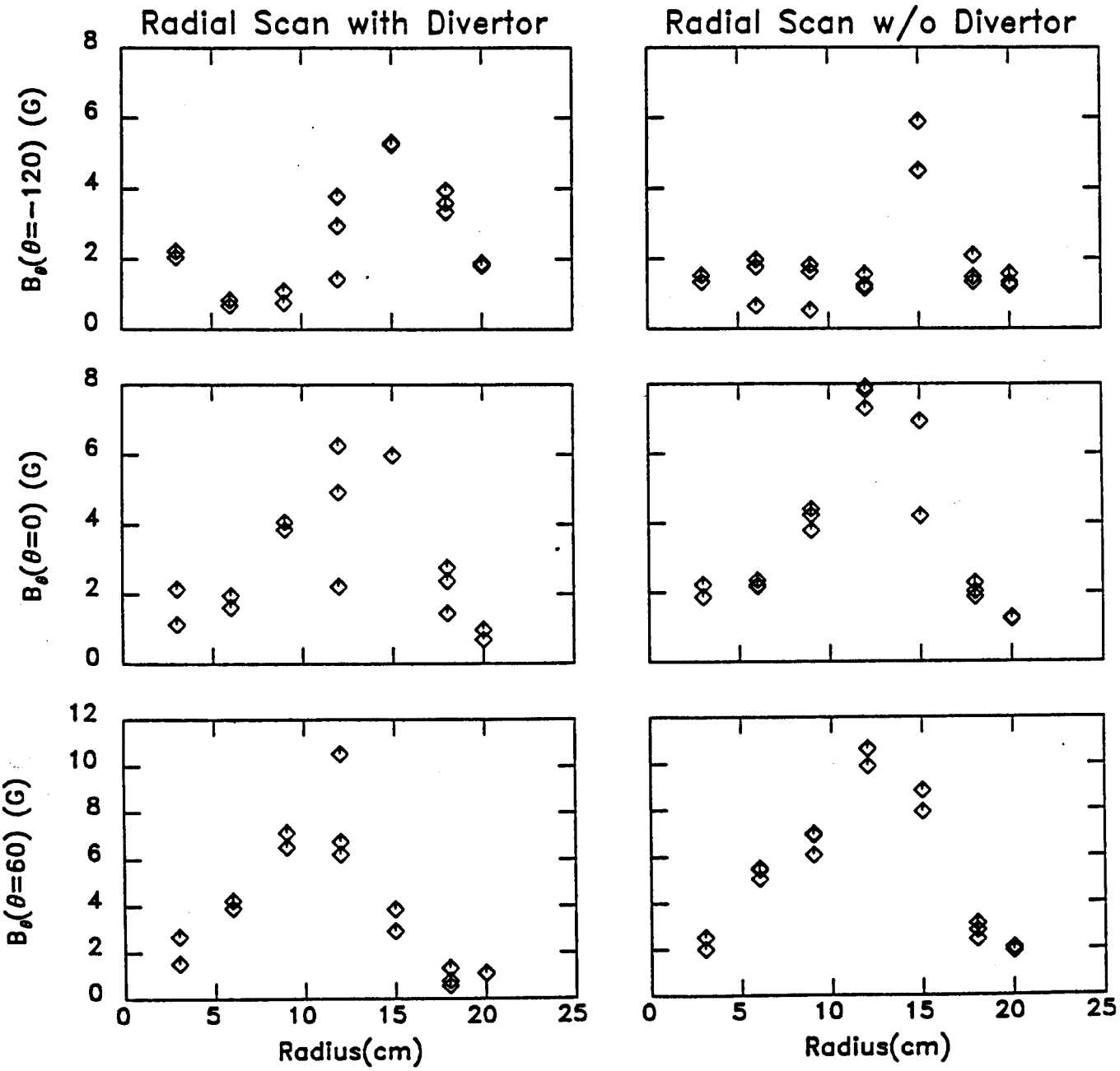
Radial Scan with Divertor
Radial Scan w/o Divertor
$B_\phi(\theta=-120)$ (G)
$B_\phi(\theta=0)$ (G)
$B_\phi(\theta=60)$ (G)
Radius(cm)
Radius(cm)

Figure 4

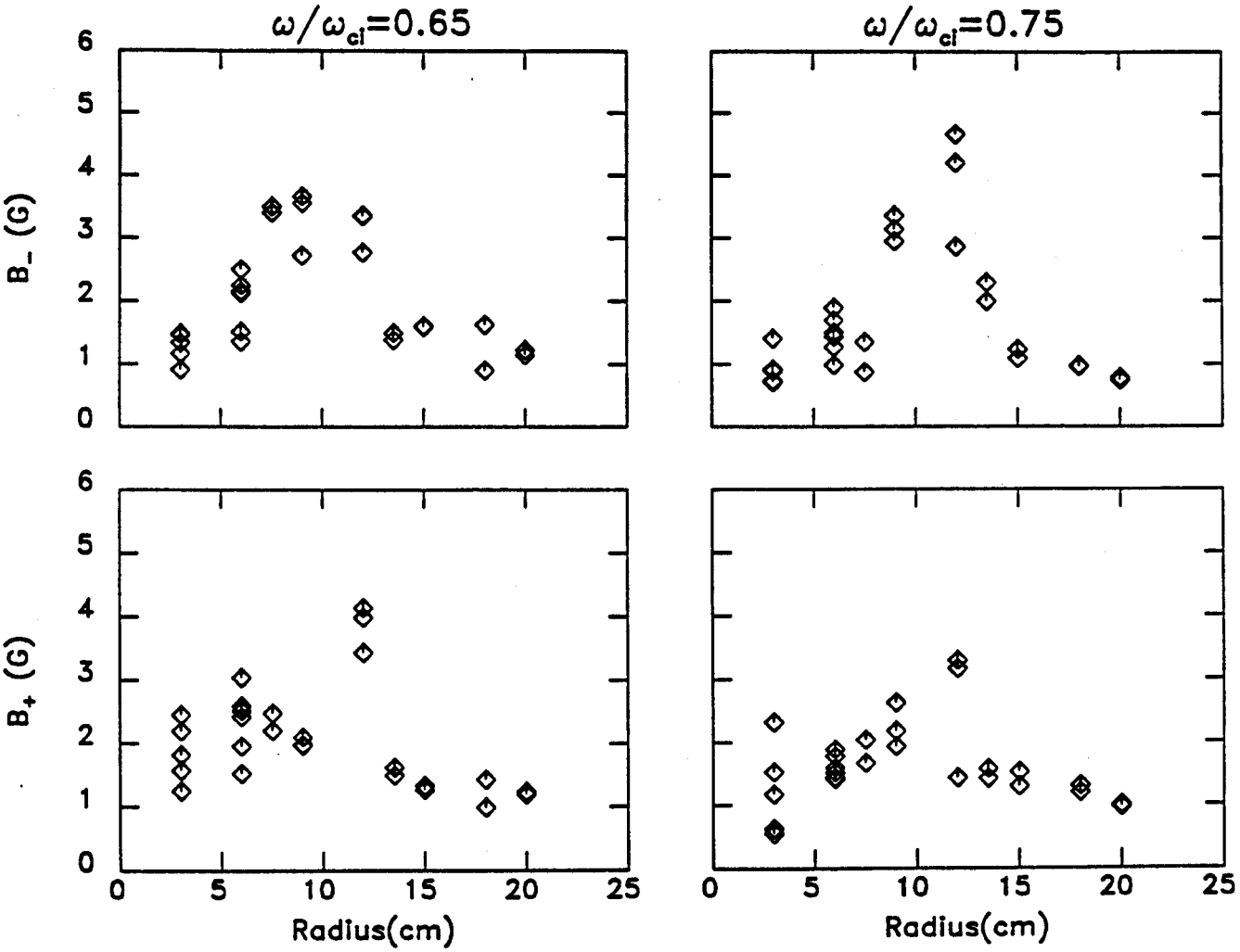

Figure 5

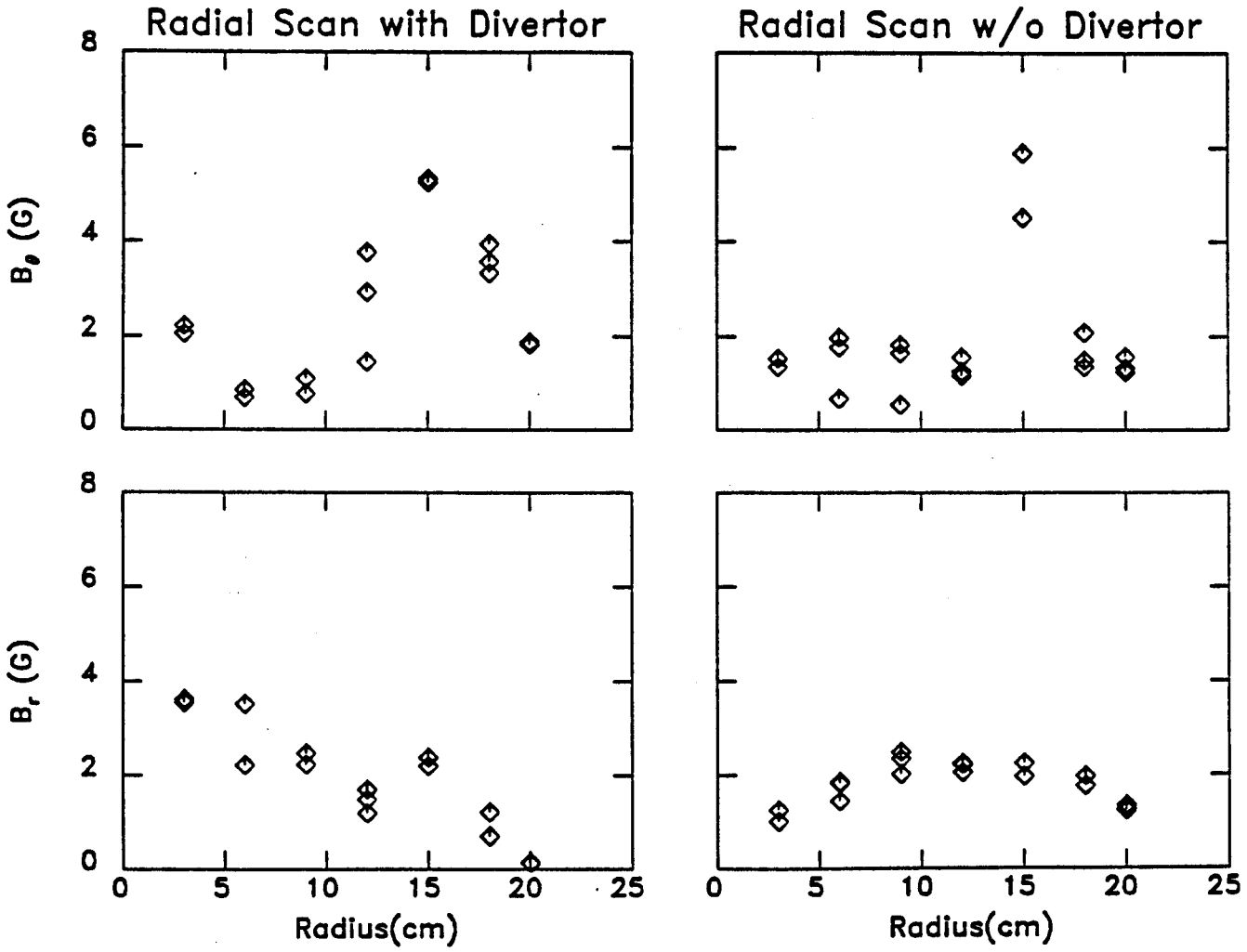
Radial Scan with Divertor
Radial Scan w/o Divertor
B_θ (G)
B_r (G)
0
2
4
6
8
0
5
10
15
20
25
Radius(cm)
Radius(cm)

Figure 6

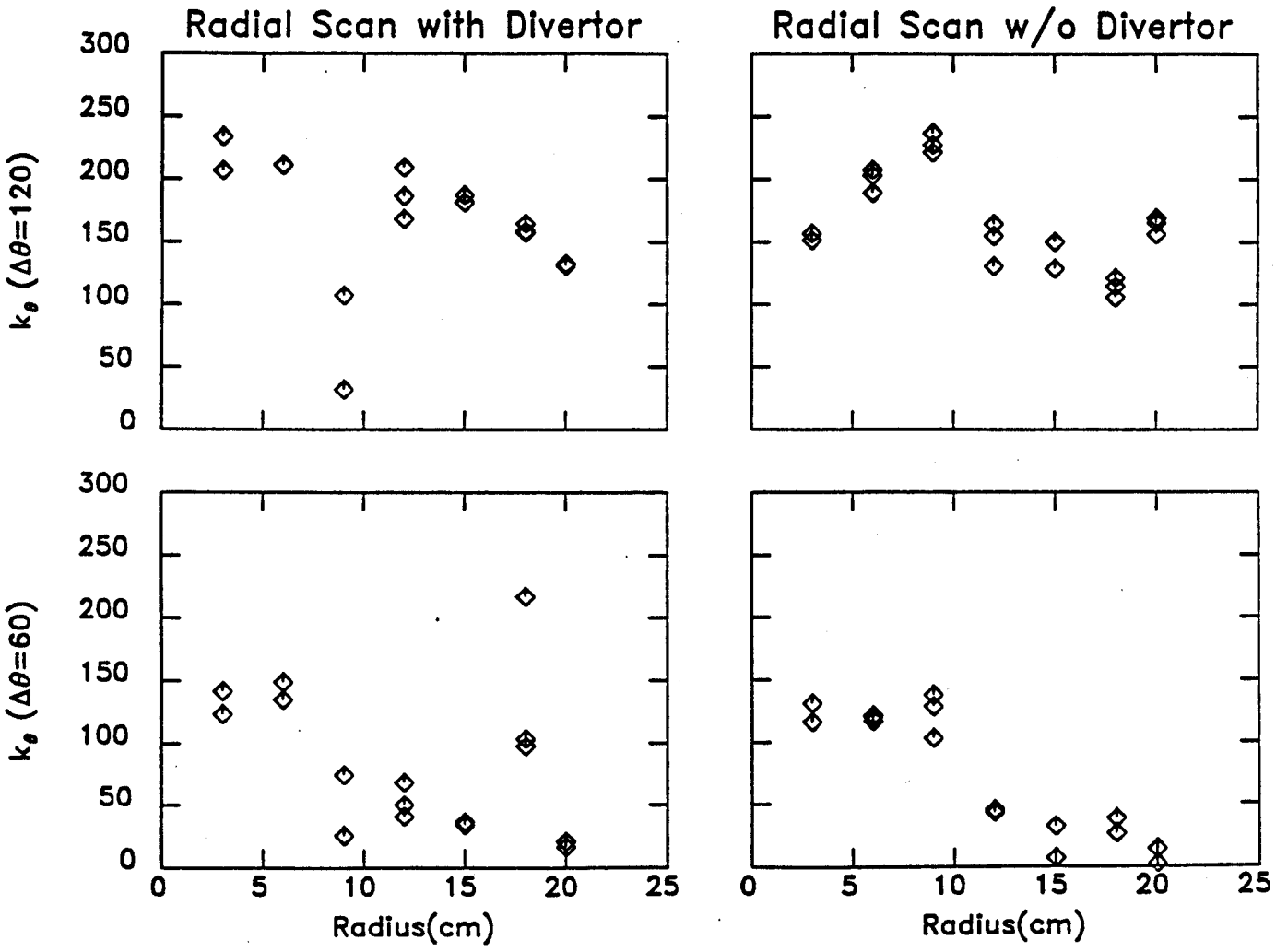
Radial Scan with Divertor
Radial Scan w/o Divertor
k_θ ($\Delta\theta$=120)
k_θ ($\Delta\theta$=60)
300
250
200
150
100
50
0
0
5
10
15
20
25
Radius(cm)

Figure 7

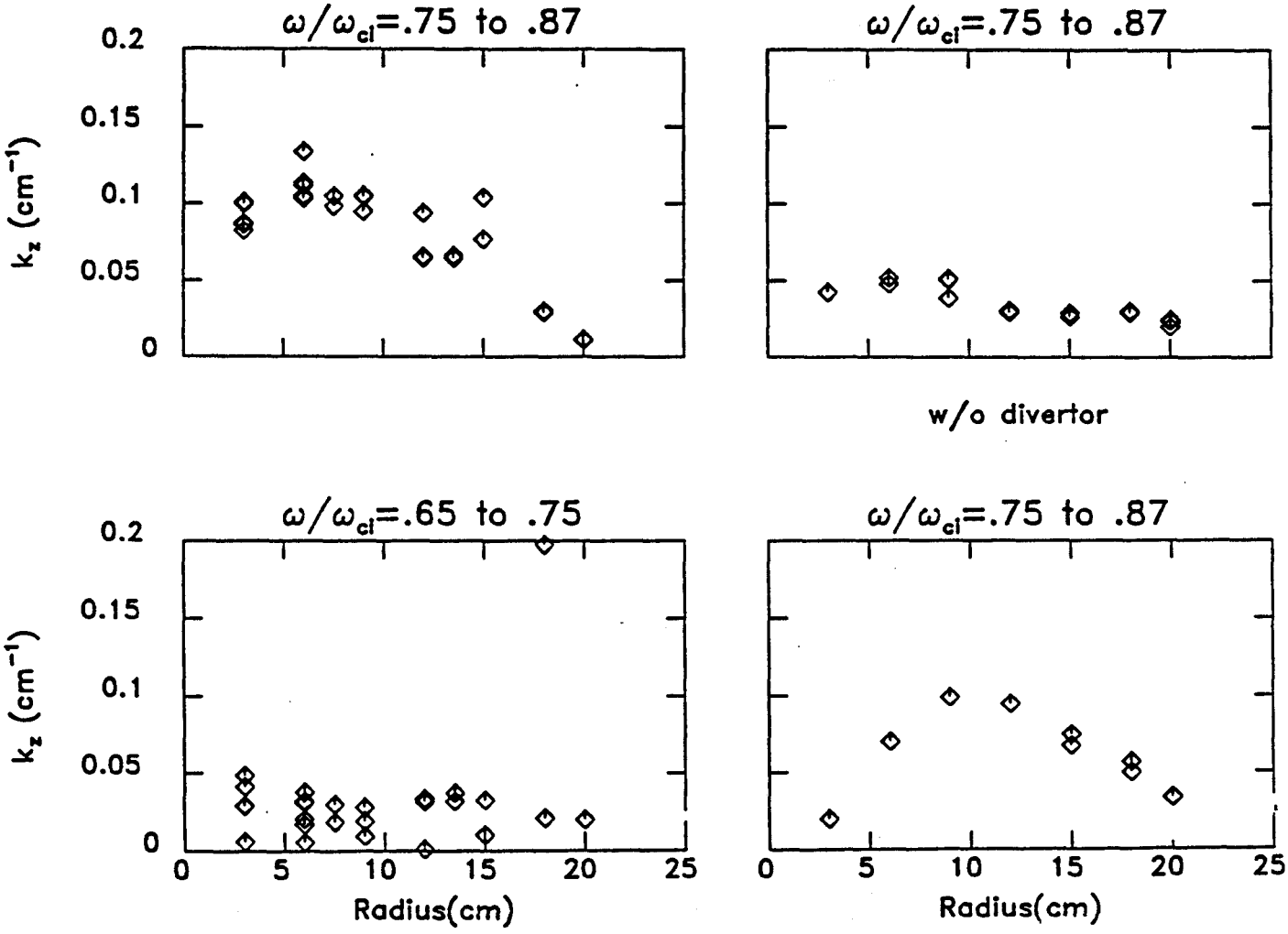
ω/ω_ci=.75 to .87
ω/ω_ci=.75 to .87
w/o divertor
ω/ω_ci=.65 to .75
ω/ω_ci=.75 to .87
k_z (cm^-1)
0.2
0.15
0.1
0.05
0
0
5
10
15
20
25
Radius(cm)

Figure 8

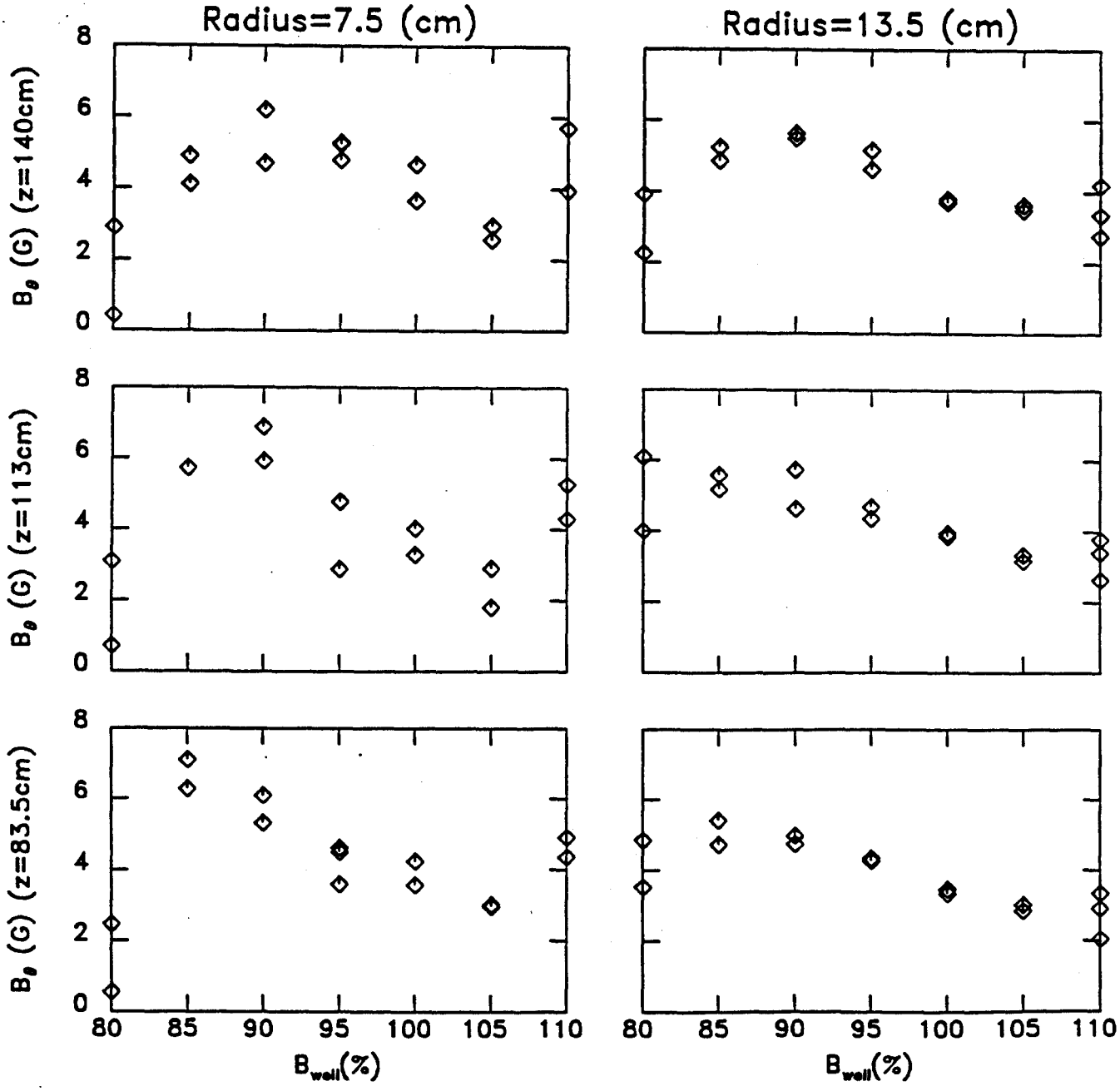
Radius=7.5 (cm)
Radius=13.5 (cm)
B_θ (G) (z=140cm)
B_θ (G) (z=113cm)
B_θ (G) (z=83.5cm)
0
2
4
6
8
80
85
90
95
100
105
110
B_{wall}(%)

Figure 9

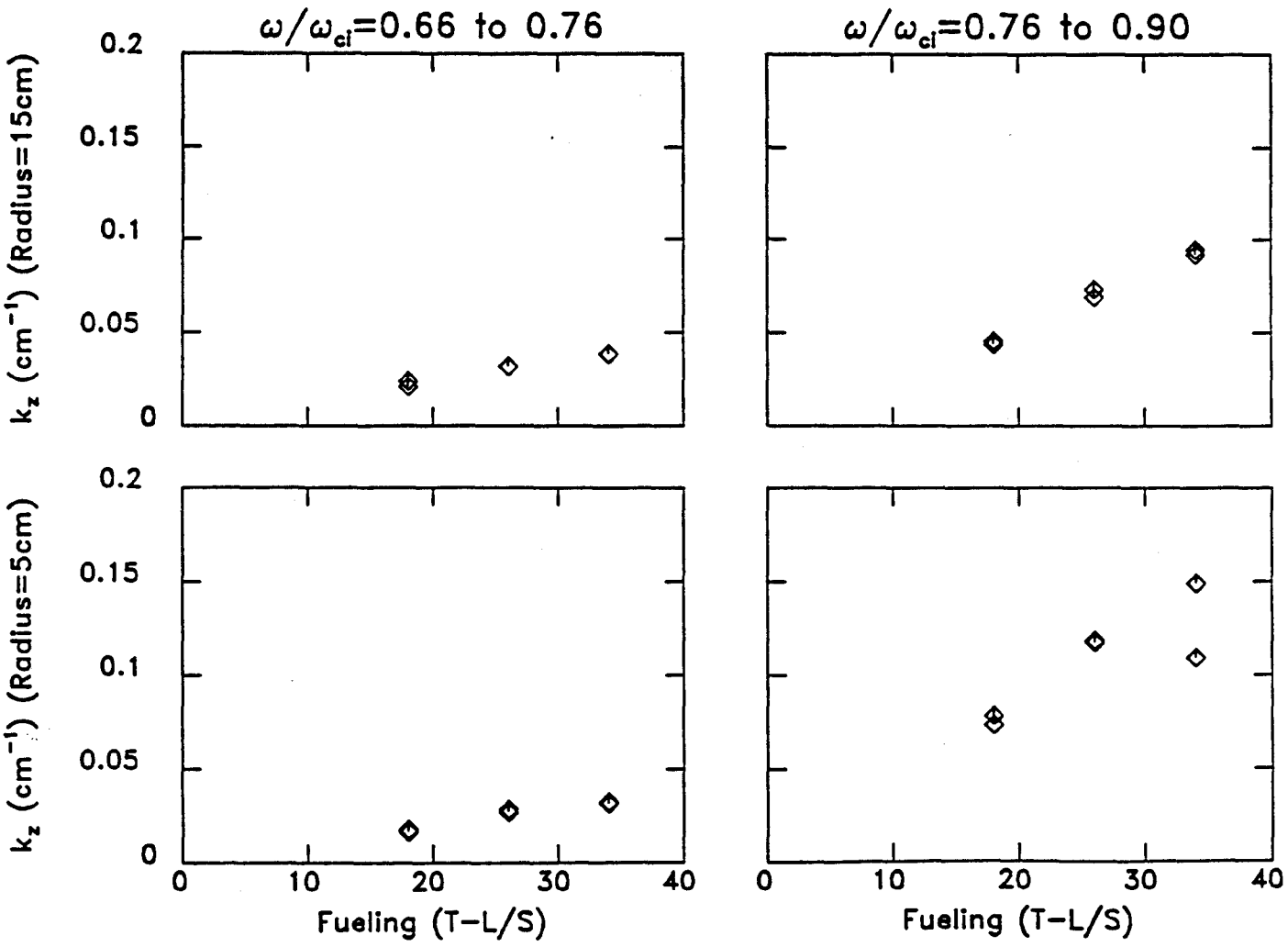
ω/ω_ci=0.66 to 0.76
ω/ω_ci=0.76 to 0.90
k_z (cm^-1) (Radius=15cm)
k_z (cm^-1) (Radius=5cm)
0.2
0.15
0.1
0.05
0
0
10
20
30
40
Fueling (T-L/S)

Figure 10